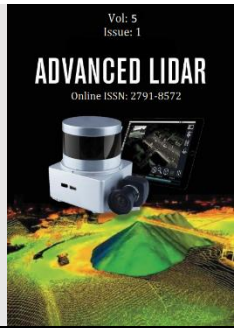
Advanced LiDAR
https://yakarm.com/journals/lidar
e-ISSN: 2791-8572
Volume 5, Number 1, pages 49–64



Research Article /Review Article:

Three Dimensional Measurement of Terrain Surfaces Slopes and Complex Geometries Using Terrestrial Laser Scanning

Hacı Murat Yılmaz *
Aksaray University, Faculty of Engineering, Department of Geomatics Engineering, Aksaray, Türkiye
* Correspondence: hmyilmaz@aksaray.edu.tr

Article History:
Received: 09.08.2025
Revised 1: 09.10.2025
Revised 2: 14.10.2025
Published: 23.10.2025

Keywords:
Point cloud;
Survey design;
Surface reconstruction;
Change detection;
Measurement uncertainty.

This article is an open-access article distributed under the terms and conditions of the Creative Commons Attribution 4.0 International License (CC BY).

Publisher's Note:
This Journal remains neutral with regard to jurisdictional claims in published maps and institutional affiliations.

Abstract

Terrestrial laser scanning provides dense three-dimensional observations of visible surfaces, but engineering reliability depends on the complete measurement chain. This technical article explains how ranging principles, angular sampling, scan geometry, registration, classification and surface reconstruction are connected when measuring terrain, slopes and complex objects. A task-based workflow distinguishes bare-earth terrain models from full three-dimensional rock-face and object representations. It identifies the role of independent control, withheld checkpoints, surface-normal comparisons and explicit treatment of occlusions. Analytical examples demonstrate the effects of oblique incidence on point spacing, vertical bias on volume estimation and uncertainty on change detection. These examples are calculated scenarios and do not represent a new field experiment. The central outcome is a reproducible approach in which model acceptance depends on coverage, reference-system consistency, geometric fidelity and independently assessed uncertainty. The article clarifies why point count and internal registration residuals alone cannot establish product accuracy, and explains how complementary surveying and imaging methods can extend coverage when their observations are controlled and verified.

Copyright © 2025 by the author(s).

Contribution to the field statement:
A task-based measurement framework links scanner observations to terrain, slope and complex-object models through explicit coverage, representation and uncertainty checks. It distinguishes analytical examples from field results and identifies the evidence required to accept each engineering product.

Highlights:
- Scan geometry controls useful surface sampling.
- Overhangs require a full three-dimensional representation.
- Independent checks test the final engineering product.
- Change detection requires an explicit uncertainty threshold.

Cite this article?
Yılmaz, H. M. (2025). Three dimensional measurement of terrain surfaces slopes and complex geometries using terrestrial laser scanning. Advanced LiDAR, 5(1), 49–64.

Technical Article

1. INTRODUCTION

Terrestrial laser scanning (TLS) measures the geometry of visible surfaces through repeated observations of range and direction from a stationary instrument. The resulting point cloud makes it possible to interrogate a surface after fieldwork, extract sections at different positions and construct geometrical models at a level of detail selected for the engineering task. Its usefulness for civil engineering derives from this connection between spatial measurement and model production, rather than from point count alone. Terrain, slopes and complex objects require different sampling and representation strategies even when the same scanner is used.

The essential measurement problem is to obtain a surface that is sufficiently complete, accurately positioned and appropriately represented for its intended analysis. On a terrain surface, vegetation removal and preservation of breaklines are central. On a steep slope, viewing geometry and the identification of stable reference areas become

decisive. On a complex structure, recesses, thin members and multiple surfaces along the same vertical line make a conventional elevation grid inadequate. This article explains how measurement physics, survey design, registration, modelling and verification operate together to address these problems.

The practical basis extends from irregular coastal rock surfaces to built objects. The sea-cliff modelling work of Alptekin, Çelik and Yakar provides an application context for steep natural surfaces [1]. Such applications motivate a common technical workflow, but they do not establish a universal accuracy for every scanner, surface or project.

The objective is to explain TLS as an engineering measurement technology and derive a reproducible route from a survey specification to a verified three-dimensional product. The article is a technical exposition supported by published applications and explicitly labelled analytical examples. It does not report a new field campaign, compare instruments experimentally or conduct a systematic literature review. Its contribution is a task-based explanation linking observability, sampling, geometric representation and uncertainty to the acceptance of terrain, slope and complex-geometry deliverables.

2. METHOD

The method is organised around measurement and survey design, point cloud processing, surface reconstruction and independent validation. The following subsections specify the observation models and processing decisions used to derive engineering products. The worked calculations are reported separately in Results and do not represent measurements from a new field campaign.

2.1. Measurement principles and survey design

2.1.1. Range measurement and Cartesian coordinates

A TLS instrument combines a ranging unit, angular encoders, a scanning mechanism, internal timing and processing, and an instrument reference frame. An integrated or external camera may supply colour. The measured quantities are not automatically a finished map: each return first belongs to the scanner coordinate system. A project coordinate system requires an independently defined reference network or a documented local datum. Active laser illumination permits geometric acquisition without dependence on photographic texture, although atmospheric conditions and surface optical properties still influence the return.

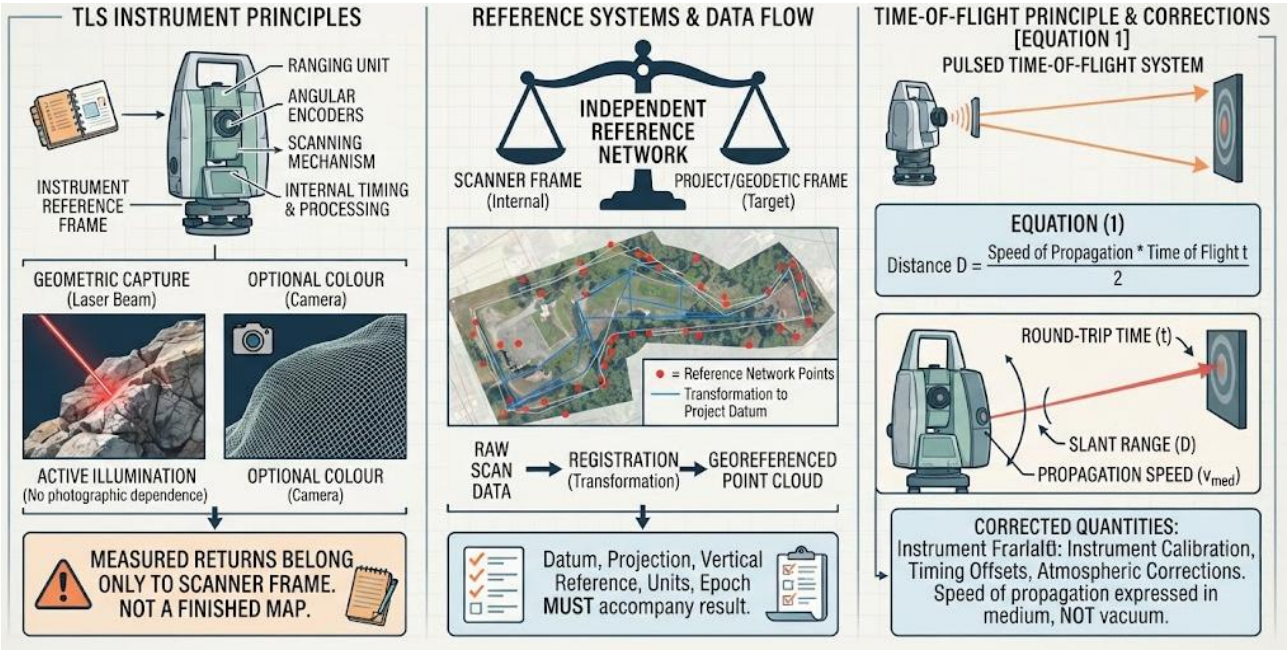


Figure 1: Best Practice Framework for Terrestrial Laser Scanning (TLS) Acquisition.

For a pulsed time-of-flight system, Equation (1) relates the measured round-trip travel time to slant range. Instrument calibration, timing offsets and atmospheric corrections are implicit in the corrected quantities used here. The speed of propagation is expressed in the surrounding medium rather than assumed to equal the vacuum speed exactly.

$$r = \frac{c_0 \, \Delta t}{2n} \quad (1)$$

Here r is range in metres, c_0 is the speed of light in vacuum, Δt is the corrected round-trip travel time in seconds and n is the refractive index of the medium. A phase-based system instead estimates the phase difference of an amplitude-modulated signal. For one modulation frequency, Equation (2) expresses the relationship within a single ambiguity interval.

$$r = \frac{c_0 (\Delta\varphi + 2\pi k)}{4\pi n f} \quad (2)$$

In Equation (2), f is modulation frequency, Δφ is phase difference in radians and k is an integer ambiguity. Multiple frequencies or other ranging information are required to resolve ambiguities over a useful measurement interval. Pulsed and phase-based systems should therefore be selected by verified range, uncertainty, return behaviour and operating conditions, rather than by a generic claim that one principle is always superior.

Let θ denote horizontal direction and α elevation above the instrument horizontal plane. Equation (3) transforms the polar observations into the scanner frame, with a right-handed axis convention defined in the survey metadata.

$$x = r \cos\alpha \cos\theta; \quad y = r \cos\alpha \sin\theta; \quad z = r \sin\alpha \quad (3)$$

The transformation makes clear why angular uncertainty becomes important at increasing range: an angular error acts over a longer lever arm. Instrument tilt compensation, levelling, target-centre determination and mechanical stability contribute additional uncertainty. A dense cloud may look smooth while retaining a systematic displacement or tilt; visual realism alone does not verify the coordinates.

2.1.2. Angular sampling and surface footprint

Angular step determines the spacing of neighbouring rays. For a small angular increment Δψ and a locally planar surface viewed close to normal incidence, the approximate spacing is rΔψ. At oblique incidence, the spacing and the laser footprint increase in the direction of surface inclination. Equation (4) provides a local planning approximation for that direction, where i is the angle between the ray and the surface normal.

$$s \approx \frac{r\,\Delta\psi}{\cos i}; \quad d(r) \approx d_0 + \beta r \quad (4)$$

Here s is surface spacing, d_0 is an approximate initial beam diameter and β is full-angle beam divergence expressed in radians. The second expression is a simplified propagation model, not a substitute for a manufacturer's calibrated beam definition. Surface roughness, receiver response and partial illumination of an edge further affect the measured point. Sample spacing and beam footprint are different quantities: decreasing the angular step cannot recover a feature smaller than the effective resolving capability of the measurement.

Figure 1 illustrates why slope orientation changes the effective measurement geometry. At grazing incidence, shadow zones, enlarged footprints and mixed returns become more likely. A scan station located opposite a face may be more useful than a closer station looking almost parallel to it. The same principle explains why roofs, slope crests and recesses often require additional viewpoints.

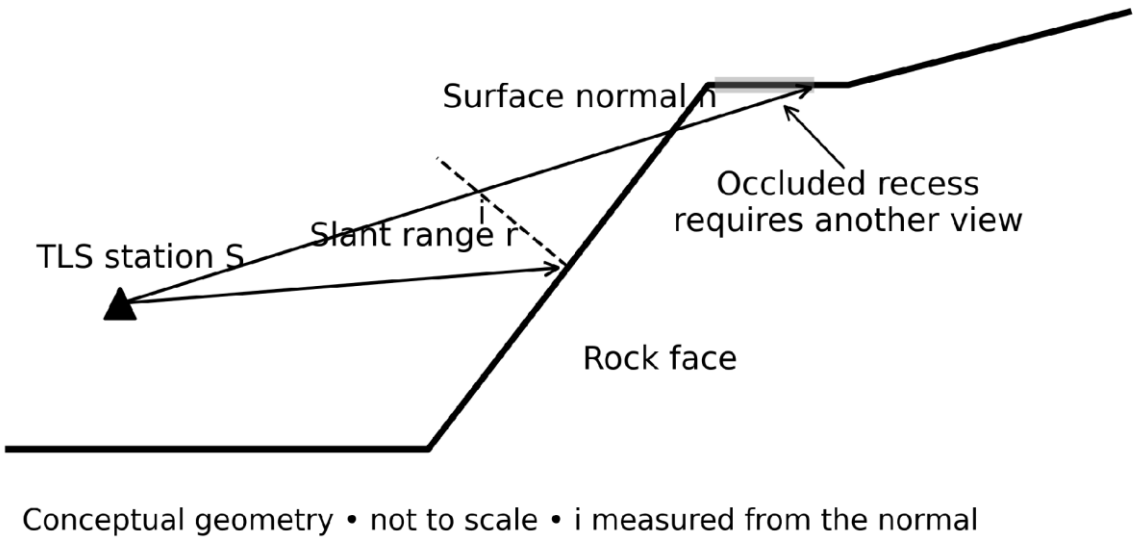


Figure 2. Range, incidence angle and visibility in a conceptual slope survey

As a calculated planning example, assume r = 50 m and $\Delta\psi$ = 0.02° = 0.0003491 rad. Equation (4) gives approximately 17.5 mm spacing at normal incidence and 34.9 mm at i = 60°. These values describe sampling under the stated assumptions; they are not observed coordinate errors. If the assumed beam divergence is 0.3 mrad and the initial diameter is neglected, the divergence contribution to diameter is 15 mm at 50 m. A requested millimetre-scale feature cannot be justified simply because software displays a millimetre coordinate precision.

2.1.3. Selection of the measurement system

Static TLS is particularly appropriate when the object is stable during acquisition, station positions can be established safely and geometric control is important. Wearable mobile LiDAR introduces a moving trajectory and simultaneous localisation and mapping into the observation chain. The book by Yakar and Karabacak explains the wearable platform and its applications [2]. The reported misuse examples at Soli Beach and the Ankara National Library underpass reinforce the importance of appropriate acquisition geometry and operational practice [3]. They should not be interpreted as field validation of static TLS.

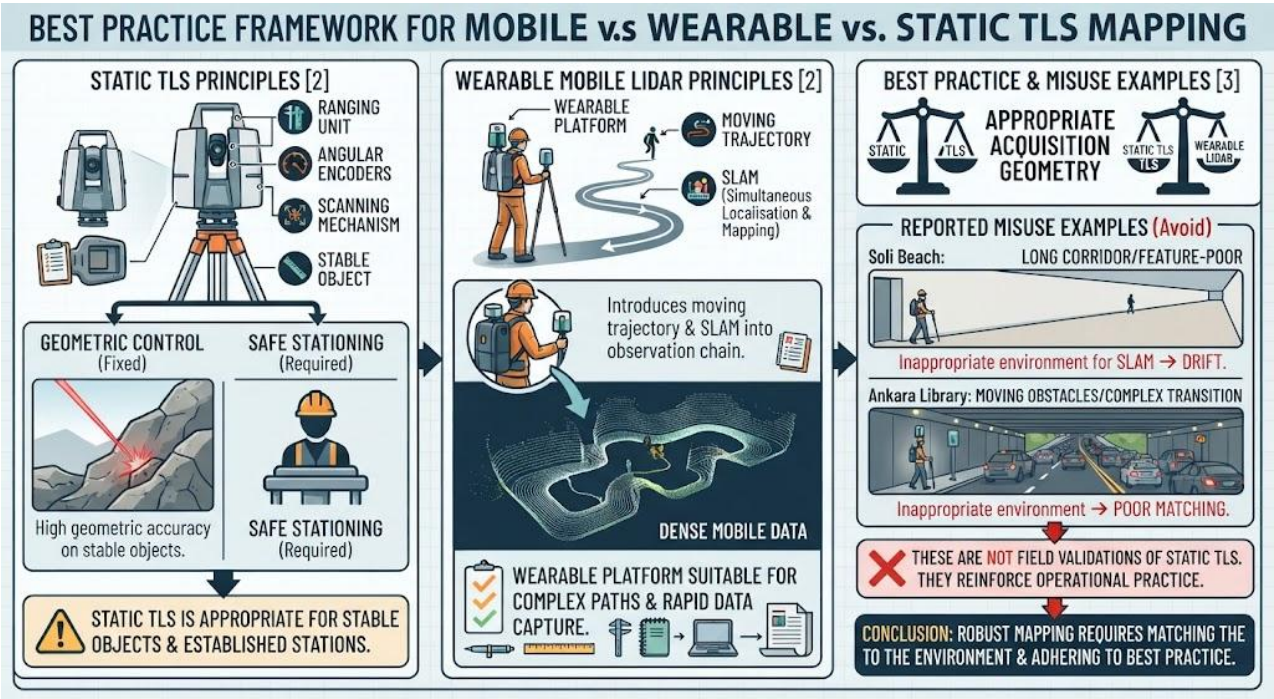


Figure 3: Best Practice Framework for Acquisition Geometry and Misuse Examples.

Metrology-grade handheld scanners, smartphone depth sensors and SLAM-based mapping systems are distinct measurement systems. Dörtbudak and Akça provide an application context for smartphone LiDAR and photogrammetric documentation [4]. The engineering consequence is to verify each system against the required measurand, working distance and uncertainty; the shared term LiDAR does not imply interchangeable performance.

Table 1 connects the three target classes to their acquisition and modelling requirements. Platform selection should follow this specification. A scanner with a very high nominal measurement rate may still fail if its useful range, beam characteristics or available viewpoints do not resolve the critical surfaces.

Table 1. Measurement and representation requirements by target class

Target	Primary observations	Preferred representation	Critical verification
Terrain	Bare ground and breaklines	Elevation grid or TIN	Ground classification; elevations; boundary
Steep slope	Face, crest, toe and discontinuities	3D mesh and local surface patches	Occlusion; stable datum; change uncertainty
Complex object	Connected surfaces and critical dimensions	Mesh, fitted primitives or parametric model	Thin features; curvature; fitting residuals

2.1.4. Control network and station configuration

The first survey decision is the definition of the measurand: terrain elevation, slope displacement, excavated volume, object dimensions or surface condition. The specification then states reference system, units, coverage, minimum feature size, uncertainty tolerance and required products. For a slope, stable control must be located outside the expected deformation zone. For long or irregular sites, reference observations should constrain the whole network rather than only one end. Target locations should offer three-dimensional spread, reliable visibility and a practical route for independent coordinate measurement.

Survey control and validation points serve different purposes. Control contributes to orientation or adjustment; checkpoints are withheld from those operations. At least three non-collinear, correctly identified point correspondences geometrically constrain a rigid transformation, but this is only a minimum configuration. Redundant, spatially distributed targets improve detectability of mistakes and weak geometry. Coplanar or clustered control can leave some transformation components poorly conditioned, especially when the survey extends well beyond the controlled area.

The total-station modelling study of Yıldız and colleagues is relevant because a scanner does not remove the need for conventional geometric control [5]. Target positions measured by total station or GNSS must carry their own uncertainty and datum information. Coordinates obtained from GNSS and scanner heights must use a consistent vertical reference; an ellipsoidal height is not automatically the engineering elevation used in a design surface.

Station planning is a visibility problem. Each critical surface should be observable from a useful direction, adjacent scans should share stable geometric features or targets, and important transitions should receive redundant observations. Koca and Kozlu discuss practical advantages and disadvantages of TLS in a monumental church [6]. Albayrak and Büyükmıhcı document a survey involving carved pigeonry spaces [7]. These geometries show why internal cavities and linked spaces require stations that follow the object configuration rather than a uniformly spaced line of instruments.

2.1.5. Field acquisition and completeness checks

Before acquisition, the operator checks instrument condition, calibration information, tripod stability, levelling, target installation and clock settings. Scan resolution is selected at the expected working distance, with closer attention to crests, toes, discontinuities, narrow members and transitions. Exposure settings for photographs should be recorded separately from ranging settings. The instrument's laser safety classification and operating instructions apply throughout fieldwork, and stations should be placed without entering unstable ground.

During scanning, moving vegetation, vehicles, pedestrians, rain, dust and reflective or transparent surfaces may introduce incomplete or unreliable returns. Wet rock can differ from dry rock in its optical response. A dark surface may provide fewer usable returns, while glass or polished metal may create misleading geometries. These areas should be flagged, examined from another viewpoint where possible and measured by a complementary method if the specification requires them.

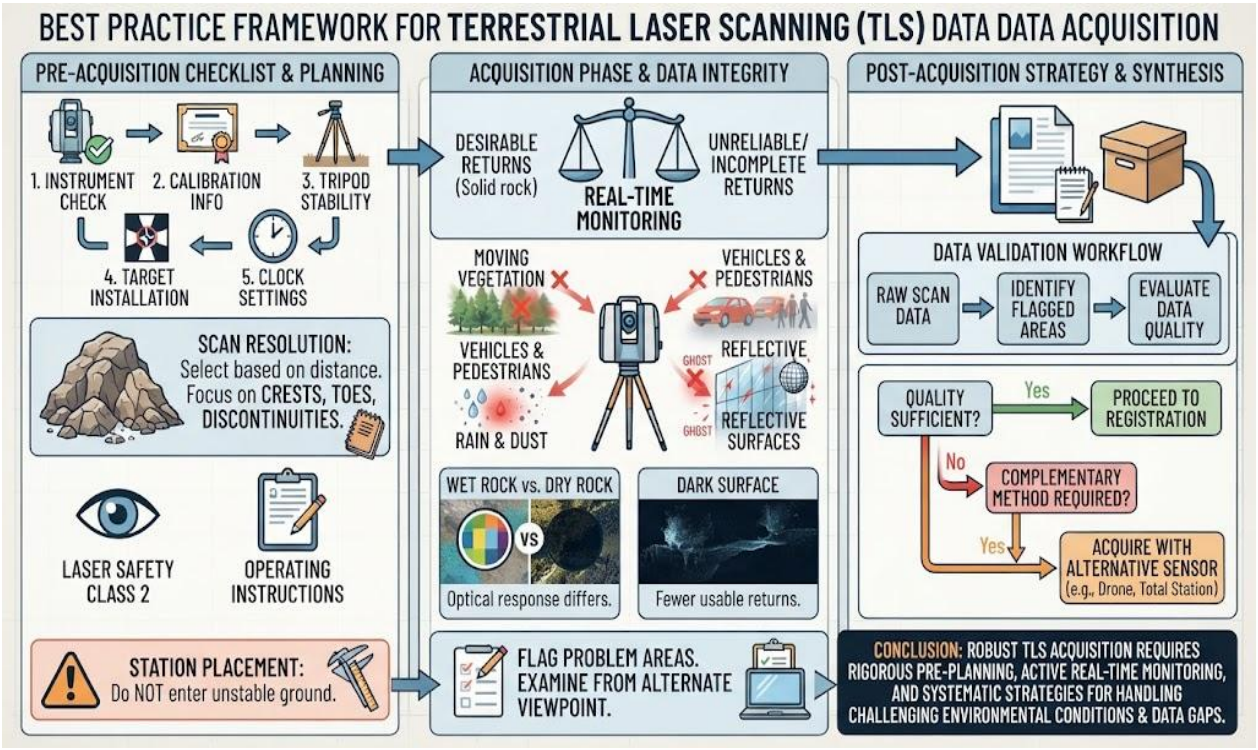


Figure 4: Best Practice Framework for Terrestrial Laser Scanning (TLS) Data Acquisition and Quality Management.

Field completeness checking uses a preliminary registration or a station coverage map. A scan count is not a coverage metric: several stations can repeatedly sample the same visible face while leaving a recess unmeasured. Güleç Korumaz's discussion of archaeological documentation limitations provides a useful reminder that method suitability depends on the actual observation conditions [8]. The deliverable should therefore distinguish observed surfaces, occluded surfaces and any modelled interpolation.

2.2. Point cloud processing

2.2.1. Import and preservation of observations

Processing begins with a protected copy of the native measurements. Station identifiers, timestamps, settings, target observations, coordinate units and instrument information are retained. A working copy may then be cleaned and reduced. Native files preserve manufacturer-specific observation information; exchange formats such as E57 can support interoperable point-cloud delivery, while LAS or LAZ may be suitable for classified point datasets when the relevant attributes are preserved. An exported mesh alone cannot reproduce the original ranging observations.

Early quality checks examine station extents, target visibility, intensity distributions and unexpected surfaces. Points on moving objects and isolated returns are candidates for removal, but aggressive cleaning can destroy valid thin objects or rough rock details. Filters should be tested on representative subsets and their settings recorded. A common voxel spacing may improve computational efficiency, but its size must remain consistent with the smallest feature that the final model must retain.

2.2.2. Registration and reference-system transformation

Registration places individual scans into a common frame. For a metric scanner whose scale is accepted from calibration, the rigid transformation in Equation (5) contains a rotation matrix R and translation vector t. A free scale parameter should not be introduced casually to improve agreement because it can conceal a calibration or unit problem.

$$p^G = R\,p^S + t \quad (5)$$

Here p^s is a point in the scanner frame and p^G is the corresponding project-frame point. A target-based solution uses observed target centres. Surface-based registration uses corresponding geometric regions, often refined with an iterative closest point (ICP) approach. Besl and McKay provide the foundational registration formulation [9].

With weights w_i and accepted correspondences between source points p_i and target points q_i, a point-to-point objective is shown in Equation (6).

$$min_{R,t} \ \sum_{i=1}^{N} \ w_i \ \|R \ p_i \ + \ t \ - \ q_i\|^2 \quad (6)$$

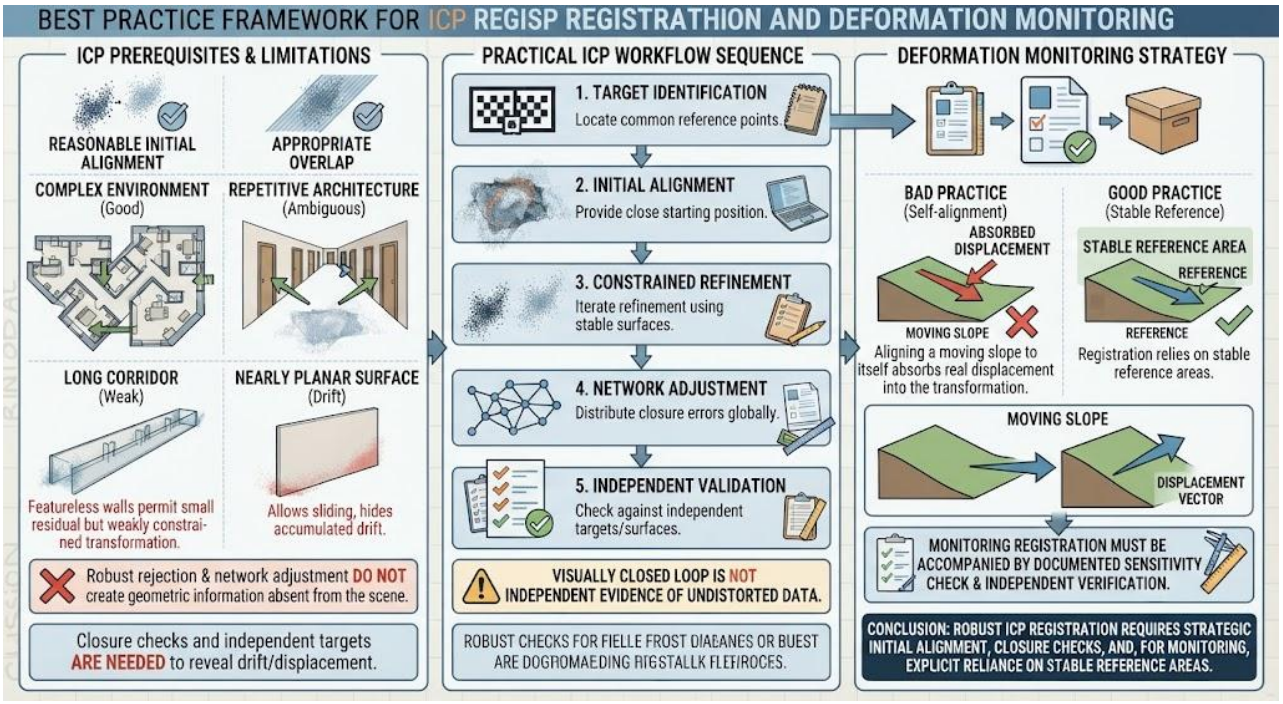


Figure 5: Best Practice Framework for ICP Registration and Deformation Monitoring.

ICP requires a reasonable initial alignment and appropriate overlap. Repetitive architecture, long featureless corridors and nearly planar surfaces may permit an apparently small residual while leaving a weakly constrained transformation. Robust rejection of invalid matches and a network adjustment reduce the effect of outliers, but they do not create information absent from the geometry. Closure checks and independently observed targets are needed to reveal accumulated drift or a common displacement.

A practical sequence is target identification, initial alignment, constrained refinement using stable surfaces, network adjustment and independent validation. The same regions must not be assumed stable when the objective is deformation monitoring. Aligning a moving slope to itself can absorb part of the real displacement into the estimated transformation. Registration for monitoring should therefore rely on stable reference areas and be accompanied by a documented sensitivity check.

2.2.3. Cleaning and semantic classification

Noise removal and object classification answer different questions. A noise filter asks whether a return is inconsistent with its neighbourhood; a classifier asks whether a valid point belongs to terrain, vegetation, structure or another class. A return on a shrub is a correct observation of the shrub even when it must be excluded from a bare-earth terrain model. Treating all non-ground returns as random measurement errors obscures this distinction.

The cloth simulation filtering approach of Zhang and colleagues is a useful example of model-based ground extraction [10]. Its parameters must reflect terrain scale and morphology. Kuçak and Büyüksalih show that ground filtering performance depends on point-cloud and terrain characteristics [11]. Sarıtaş and Kaplan further examine the sensitivity of ground extraction to selected filtering settings [12]. Their airborne-data applications inform algorithm selection, but the resulting parameter choices cannot be transferred unchanged to steep terrestrial scans.

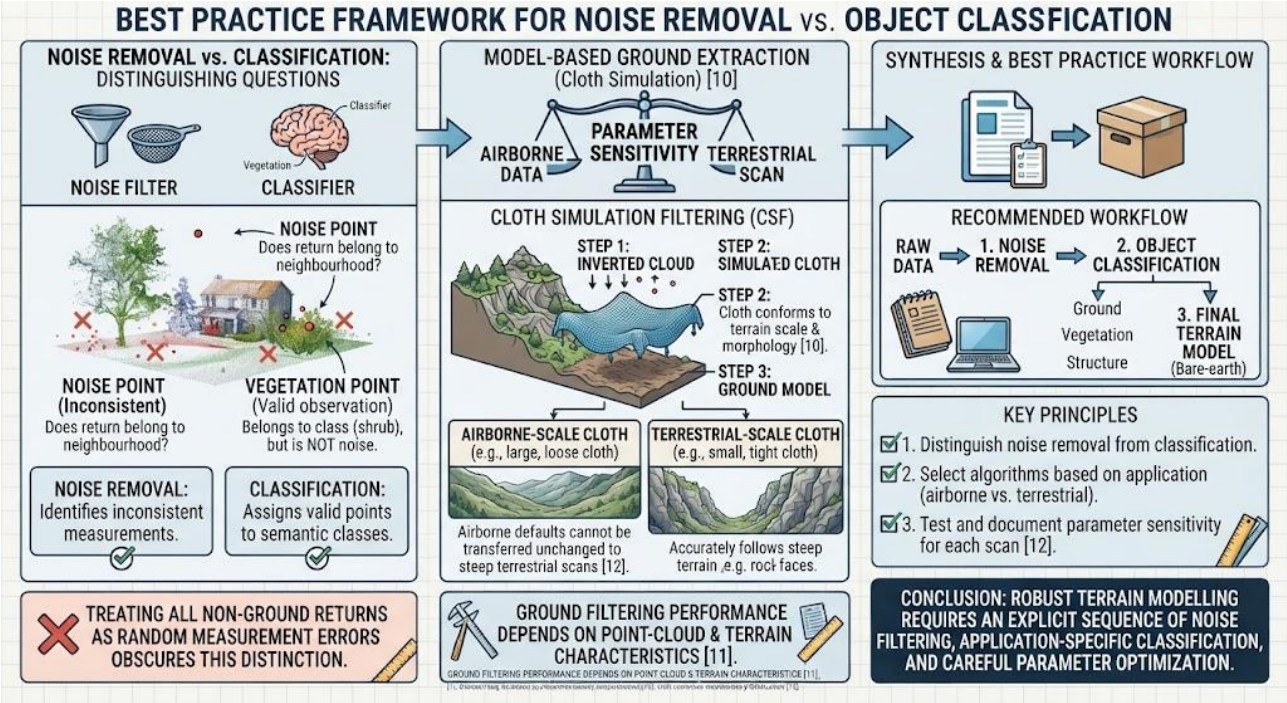


Figure 6: Best Practice Framework for Noise Removal vs. Object Classification.

On an overhanging cliff, a valid rock surface can be nearly vertical or face downward. A conventional terrain filter designed for a single-valued elevation surface may reject that geometry. Processing should therefore separate a bare-earth terrain product from a rock-face product. The slope cloud is classified using surface orientation, connectivity and geological interpretation as appropriate, with manual checking around the toe, crest and discontinuities.

Filtering also changes derived volumes. Sarıtaş and Kaplan's Skopje analysis relates ground-model construction to filtering choices [13]. For a TLS project, the corresponding check is to compare representative cross-sections before and after filtering, inspect removed points and calculate differences between accepted model variants. A visually cleaner result is not sufficient evidence that a more accurate terrain model has been produced.

2.2.4. Surface normals and geometric segmentation

Local surface analysis estimates a normal from neighbouring points, commonly through principal component analysis. A small neighbourhood preserves details but is sensitive to noise; a large neighbourhood smooths across edges and small discontinuities. Neighbourhood radius should therefore be related to point spacing, roughness and feature scale. Eigenvalue-based descriptors can help distinguish planar, linear and volumetric neighbourhoods, but their interpretation remains scale dependent.

Random sample consensus (RANSAC), introduced by Fischler and Bolles, fits models despite outliers [14]. Kuçak applies geometric features and RANSAC to extracting information from point clouds [15]. For a rock slope, a plane fit may represent a discontinuity patch; for a building, it may represent a wall. The acceptance threshold must be expressed in distance units and justified relative to roughness and measurement uncertainty. A numerically fitted plane does not itself identify a geological joint or structural defect.

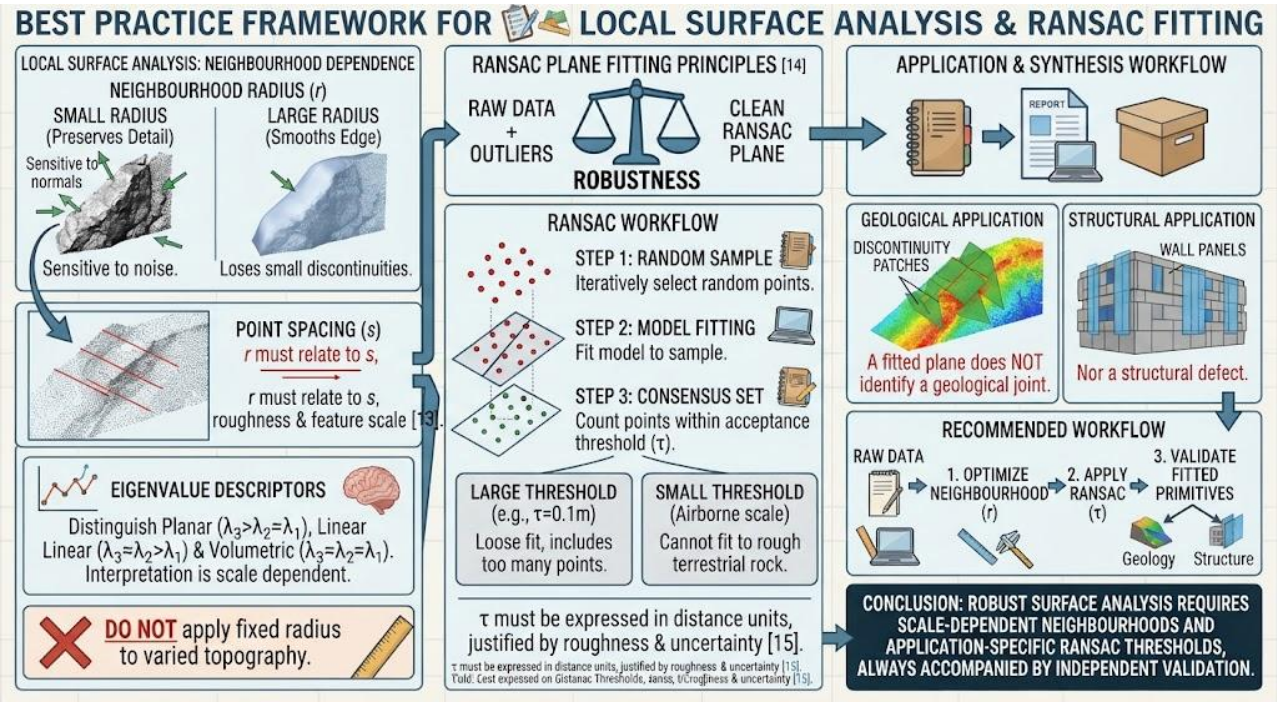


Figure 7: Best Practice Framework for Local Surface Analysis and RANSAC Fitting.

2.3. Surface modelling and engineering products

2.3.1. Terrain surfaces and volume measurement

A digital terrain model represents the bare-earth surface. A regular grid is convenient for elevation differences and raster analysis, while a triangulated irregular network (TIN) can retain variable point density and explicitly incorporated breaklines. Crest lines, drainage channels, retaining-wall edges and abrupt transitions should be represented intentionally. A small grid cell does not increase the information content of a sparse cloud and may generate unstable interpolation in occluded regions.

For a terrain that can be expressed as z = f(x,y), each horizontal position has one accepted ground elevation. A TIN or elevation raster can then support slope, aspect, contours and cut-and-fill calculations. For an overhang, several surface points may share the same horizontal location at different heights. Such geometry requires a full three-dimensional mesh or another multi-surface representation. Projecting it onto a height grid removes part of the object regardless of the grid resolution.

Before volume computation, both surfaces must use the same datum, boundary and vertical convention. Equation (7) gives a grid approximation of signed volume change over a common valid domain Ω. The cell area A_j is a horizontal projected area; cut and fill should also be reported separately where the engineering question requires them.

The TÜBİTAK project by Yakar, Yılmaz and Mutluoğlu addresses volume calculation using laser scanning and photogrammetric methods [16]. This application context is relevant to selecting a surface acquisition method for quantity estimation. In the workflow presented here, the volume remains dependent on the accepted model, its boundary and the reference surface; the numerical values in Table 2 are calculated examples rather than results from that project.

$$\Delta V \approx \sum_{j\in\Omega} A_j \,(z_{2,j} - z_{1,j}) \quad (7)$$

Boundary selection, vegetation classification and interpolation can contribute more to volume uncertainty than random point noise. Unobserved cells should be masked or assigned a clearly documented reconstruction method. For closed objects, a consistently oriented, watertight three-dimensional mesh may support an enclosed-volume calculation, but closing an unobserved base creates an assumed boundary and must be disclosed.

Table 2 presents a transparent numerical example using Equation (7). A uniform vertical bias of only 10 mm over 1,000 m^2 would contribute 10 m^3 to the estimated volume. This calculation explains why a dense surface still needs reliable datum control. It does not establish a measured TLS volume error.

Table 2. Calculated volume example over a common valid domain

Zone	Area (m^2)	Mean Δz (m)	Signed ΔV (m^3)
A	400	+0.020	+8.0
B	350	−0.010	−3.5
C	250	+0.040	+10.0
Total	1,000	—	+14.5

Assumed values only. Positive change is fill and negative change is cut relative to the first surface. Fill = 18.0 m^3; cut = 3.5 m^3; net change = +14.5 m^3.

2.3.2. Slope geometry and change measurement

For a slope, useful products include face meshes, crest and toe lines, profiles, discontinuity-plane orientations, roughness descriptors and multi-epoch change maps. The rockfall application of Abellán, Vilaplana and Martínez provides a primary example of long-range TLS applied to a steep natural face [17]. The measurement logic is to preserve the three-dimensional face, maintain a stable reference frame and distinguish actual surface change from differences caused by registration or sampling.

Yilmaz and colleagues applied terrestrial laser scanning to determining erosion rates of an earth pillar [18]. This directly connects repeated three-dimensional surface recording to geomorphological monitoring. An erosion rate must be defined with its observation interval and measured quantity, such as retreat distance per unit time or volume loss per unit time. Registration uncertainty and unobserved surface regions must be considered before attributing a difference to erosion.

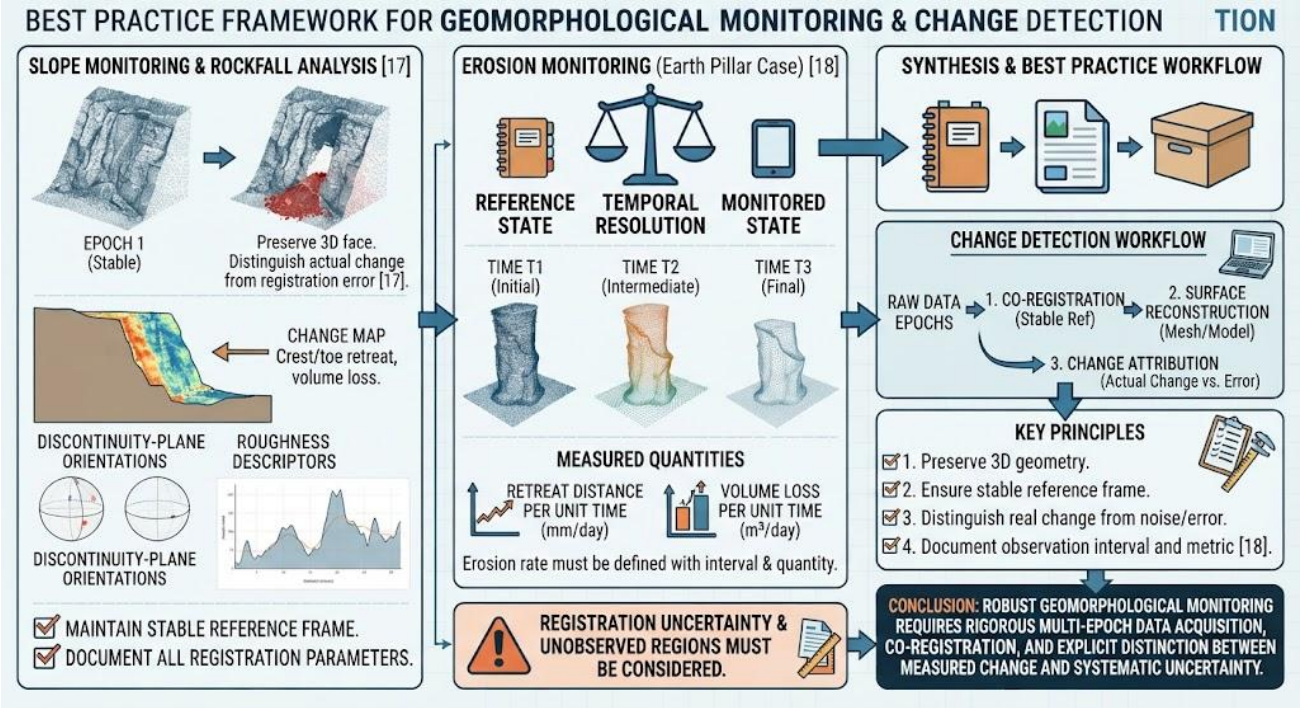


Figure 8: Best Practice Framework for Geomorphological Monitoring and Change Detection

An elevation difference is appropriate for surfaces that remain single valued and where a vertical component answers the question. It is less suitable for a near-vertical cliff because a small horizontal retreat may correspond to a very large or undefined raster elevation difference. A cloud-to-mesh or cloud-to-cloud distance along a local surface normal is often more meaningful. Lague, Brodu and Leroux developed a precision-oriented three-dimensional comparison method for complex topography [19]. Its use requires justified normal and projection scales, appropriate registration and spatially varying uncertainty assessment.

Figure 2 shows the distinction between vertical differencing and local normal distances. The normal component is a scalar change measure, not a full displacement vector. Identifying a three-dimensional motion vector additionally requires tracking corresponding material features or another observation model. Rockfall, erosion and newly exposed surfaces may violate a simple material-point correspondence, so geometric change must be interpreted with the relevant process knowledge.

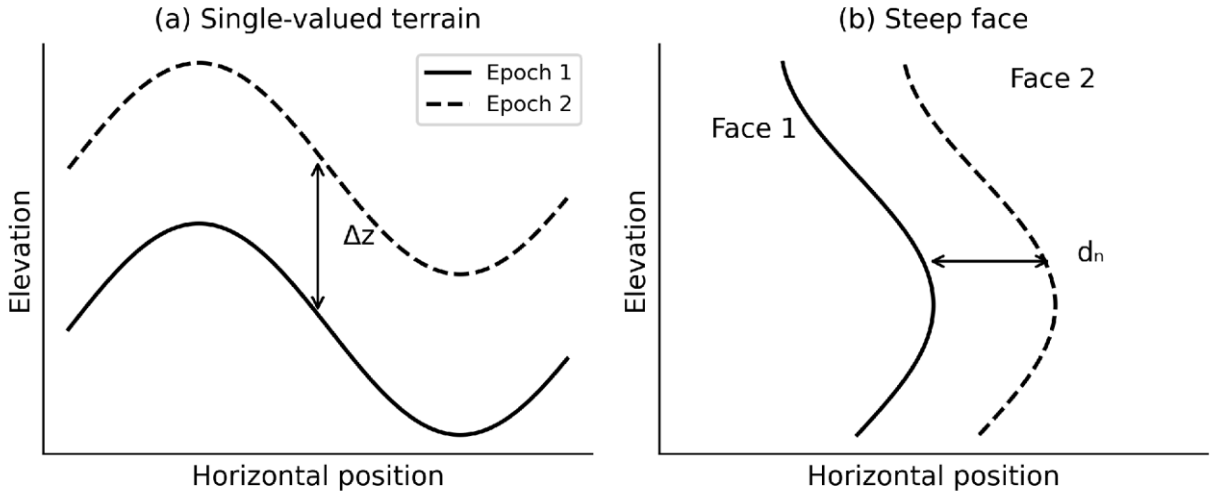


Figure 9. Terrain elevation differences and slope-normal distances represent different quantities

Multiple epochs require consistent scan geometry where practicable. Vegetation state, moisture, snow and temporary objects should be recorded because their differences can mimic change. Stable-area residuals should be mapped to test whether the registration behaves uniformly across the site. Local roughness and point density affect the minimum detectable change, so a single site-wide threshold can be misleading on a face with widely varying visibility.

2.3.3. Complex geometries and reverse engineering

Complex objects include caves, tunnels, carved interiors, irregular masonry, ships and steel structures. The principal difficulty is not only collecting many points, but maintaining surface continuity and resolving adjacent components without merging them. Promneewat and Taksavasu's profile-based cave modelling illustrates the distinction between measured sections and the surfaces interpolated between them [20]. Profile spacing is therefore an explicit limitation when reconstructing irregular cavities.

Tunnel models are usually interrogated through sections defined relative to a documented centreline or local alignment. A section extracted in a global vertical plane is not necessarily a true normal section of a curved tunnel. The section plane, sampling thickness and comparison reference must be stated before reporting clearance or convergence.

Ship hulls require a continuous free-form representation that preserves curvature while avoiding artificial flattening. Kanun, Alptekin and Yakar's ship modelling study provides an application context for TLS-based reverse engineering [21]. Surface fitting should be checked against held-out cloud regions or independent dimensions. A smooth CAD surface may satisfy modelling constraints while departing from the measured object, so fitting residuals and independent dimensional checks should accompany the final model.

Steel structures introduce narrow members, repeated profiles, occlusions at joints and reflective surfaces. Individual member straightness, joint geometry and installation tolerance require checks at the relevant scale. Mobile mapping performance should be verified independently against the dimensional tolerance required for each connection.

The main modelling options are a direct mesh, fitted geometric primitives and a parametric object model. A mesh retains measured shape with limited semantic information. Primitive fitting produces planes, cylinders or other interpretable geometries. A parametric model supports component identity and engineering attributes but introduces idealisations. Özeren and Korumaz describe a LiDAR-to-HBIM workflow [22]. The technical implication is that an information model is an interpretation of the observations; model detail and geometric fidelity must be assessed separately.

2.3.4. Documentation of irregular built surfaces

The heritage examples are useful because they contain uneven surfaces, recesses, ornament and intersecting forms. Karabork and colleagues address modelling and visualisation with laser scanning [23]. Göktepe and colleagues document the Sille Aya-i Eleni Church with laser technology [24]. These applications support the use of multiple views and coherent three-dimensional documentation, without implying that geometric recording alone diagnoses material condition.

Güleç Korumaz and colleagues evaluated laser-scanner performance in documenting historical and architectural ruins in Konya [25]. Irregular ruins provide a relevant setting for the acquisition strategy discussed here because deformation and material loss can obscure an idealised geometric form. The engineering model should retain observed departures from that form when they are part of the measurand, rather than remove them automatically during fitting.

The Kanlıdivane mausoleum study by Çelik, Alptekin and Yakar provides another example of object-scale TLS documentation [26]. Köse and Us describe scanning and modelling of the Sarı İsmail Sultan Tomb [27]. For these surfaces, orthographic views and sections should be generated from a controlled model with an explicit projection direction. Colour photographs improve interpretation, but their registration and illumination should be evaluated independently of the ranging geometry.

Kanun, Metin and Yakar obtained a three-dimensional point cloud of Ağzıkara Han using terrestrial laser scanning and evaluated the combination of individual scans [28]. This application illustrates the transition from several station datasets to a unified architectural point cloud. The reported registration assessment should be distinguished from an independent test of the absolute positional accuracy of the final model.

Karataş, Alptekin and Yakar investigate material deterioration on stone façades using TLS [29]. A surface depression or loss of material may be geometrically measurable, but the cause of deterioration generally needs visual, historical or material evidence. Raw return intensity is influenced by range, incidence angle and instrument response and should not be treated as a calibrated material classification by itself.

Photogrammetry can complement TLS where fine texture or photographic detail is important. Alyılmaz, Alyılmaz and Yakar's Qobustan petroglyph study uses close-range photogrammetry [30]. It is cited here as a complementary image-based documentation method, not as a laser-scanning experiment. Kaderli discusses the documentation of Cappadocia's rock-related heritage [31], while Özdemir and Güngör consider TLS and UAV photogrammetry for archaeological excavation sites [32]. Integration requires common control and independent checking of both geometry and image alignment.

2.4. Accuracy assessment

2.4.1. Measurement uncertainty and independent validation

A TLS uncertainty budget includes ranging, angular observations, target measurement, station geometry, registration, reference control and model approximation. Some effects are random over a local patch, while others are correlated across a station or the entire project. Averaging thousands of points may reduce some random noise but cannot remove a common reference-frame bias. Accuracy should therefore be reported for the final product and the intended measurand, with the test geometry and reference uncertainty stated.

Independent checkpoints must be sufficiently well distributed to test the occupied volume, not merely a convenient cluster near the scanner. Points on ambiguous edges should be avoided unless edge behaviour itself is being tested. Where a checkpoint cannot be identified as a unique physical point in the cloud, a target centre or another reproducible geometric construction is preferable. Reference measurements should be more reliable than the required tolerance by a justified margin, with their uncertainty included in interpretation.

Let $e_{x,i}$, $e_{y,i}$ and $ez_{,i}$ be coordinate differences between the product and independent reference for checkpoint i. Equation (8) defines component and three-dimensional root mean square errors (RMSE). The mean differences should also be reported to reveal directional bias; RMSE alone combines bias and dispersion.

$$RMSE_x = \sqrt{\frac{\sum_{i=1}^{N} e_{x,i}^2}{N}}; \quad RMSE_{3D} = \sqrt{\frac{\sum_{i=1}^{N} (e_{x,i}^2 + e_{y,i}^2 + e_{z,i}^2)}{N}} \quad (8)$$

A registration residual is an internal agreement measure for the observations used by the solution. A checkpoint RMSE is an external test at the withheld checkpoint locations. A cloud-to-cloud residual is affected by sampling, surface roughness and correspondence. These measures answer different questions and should be listed separately. Reporting only the smallest one can lead to a misleading description of the final product.

Table 3 provides a compact verification framework. Acceptance thresholds must be defined from the project requirements before processing. A project may pass its checkpoint criterion but still fail completeness at the

slope crest, or pass coverage while failing a dimensional tolerance on a narrow structural member. No single summary statistic covers all such outcomes.

Table 3. Verification measures and the questions they answer

Check	Reported quantity	Interpretation
Reference control	Coordinate uncertainty and datum	Quality of the reference frame
Registration	Residuals and network closure	Internal scan agreement
Withheld checkpoints	Bias and component/3D RMSE	External positional agreement
Completeness	Coverage and occlusion mask	Presence of required surfaces
Model fidelity	Section and surface residuals	Effect of representation and fitting
Repeated surveys	Local distance and detection threshold	Change relative to uncertainty

3. RESULTS

3.1. Worked uncertainty examples

The following examples are analytical calculations using assumed inputs, not results of an acquired dataset. First, suppose five independent checkpoint differences in the vertical direction are +4, −3, +5, −2 and +1 mm. Equation (8) gives a mean difference of +1.0 mm and RMSEz = $\sqrt{(55/5)}$ = 3.32 mm. Five points are sufficient for this arithmetic demonstration but do not establish adequate validation coverage for a real site.

Second, an assumed angular standard uncertainty of 20 arcseconds equals approximately 0.00009696 rad. Its transverse contribution at 50 m is approximately 4.85 mm. If an independent range contribution of 2 mm acts in the simplified two-component model, the root-sum-square is approximately 5.25 mm. This result is an illustrative local uncertainty magnitude, not a full three-dimensional instrument specification; actual coordinate propagation requires the observation Jacobian and covariance matrix.

For repeated measurements, a simple screening threshold can be calculated from independent one-standard-deviation uncertainties u_1 and u_2 in the measured normal component and a separate relative-registration contribution u_r. Under a Gaussian approximation, Equation (9) gives a two-sided 95% threshold. Registration must not be counted again if it is already included in u_1 and u_2.

$$LoD_{95} = 1.96\sqrt{u_1^2 + u_2^2 + u_r^2} \quad (9)$$

Assume u_1 = u_2 = 4 mm and u_r = 3 mm, with all terms independent and expressed as one-standard-deviation uncertainties. Equation (9) gives approximately 12.6 mm. An observed normal distance of 8 mm would not exceed this illustrative threshold, whereas 20 mm would. The comparison does not prove a physical cause or guarantee detection over the whole slope. Spatial correlations, roughness and varying visibility require a more complete local analysis for operational monitoring.

3.2. Representation error and model sensitivity

Model sensitivity can be assessed by producing a small number of justified alternatives: different ground-filter settings, mesh edge limits, grid sizes or fitting neighbourhoods. The purpose is to reveal whether the engineering output remains stable under reasonable processing choices. Every alternative should use the same valid domain and reference frame so that a change in processing is not confused with a change in boundary or datum.

For terrain, compare breakline continuity, checkpoint elevations and cut-and-fill differences. For a slope, compare normal orientations and distances around discontinuities and shadow boundaries. For complex geometry, inspect thin elements, curved surfaces and junctions through measured sections. Difference maps should include masks for unobserved regions. An interpolation that fills a hole must not be presented as an additional measurement.

Figure 3 summarises the full workflow and locates the independent verification step. Failure at a verification gate leads back to the relevant field or processing stage. This arrangement makes a survey reviewable because a rejected surface can be traced to a visibility problem, a reference-frame weakness or a modelling decision rather than treated as an unexplained software discrepancy.

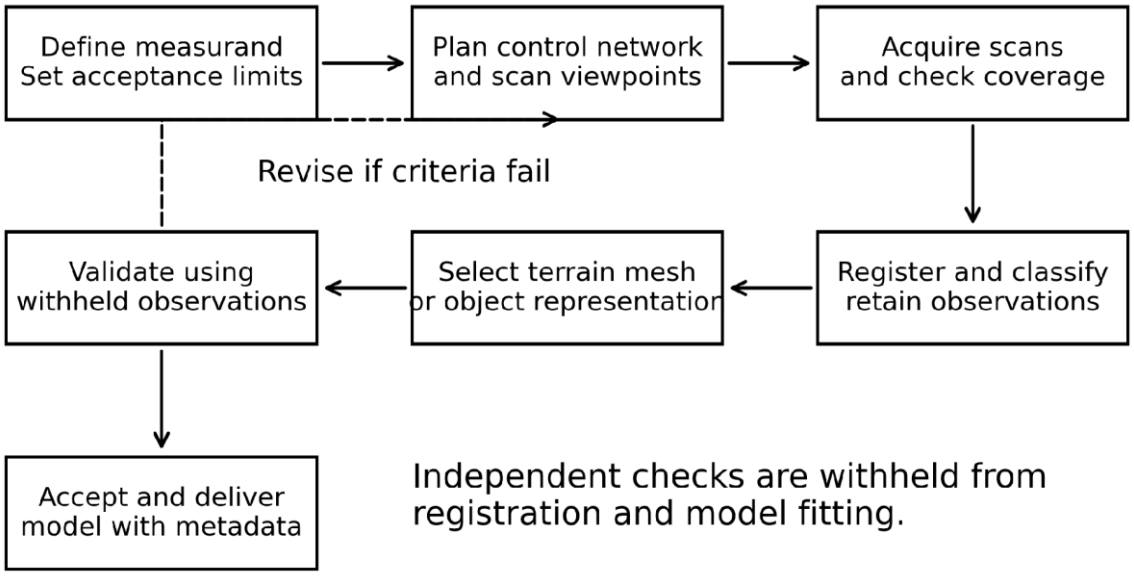


Figure 10. Task-based TLS workflow with independent verification and traceable revision

4. DISCUSSION

The most useful distinction among terrain, slopes and complex geometries is the relationship between visibility and representation. Terrain modelling commonly seeks a single bare-earth elevation. Rock-face modelling seeks a three-dimensional surface with discontinuities and possible overhangs. Complex-object modelling seeks connected surfaces and sometimes identifiable components. The same registered cloud may support all three, but it must be processed with different assumptions. A universal filtering and meshing preset is therefore unlikely to preserve every required feature.

Survey design should treat useful point density as a result of range, incidence and occlusion. Very dense scans from one station can be less informative than a coarser multi-station acquisition that resolves previously hidden faces. Conversely, adding stations without a coherent control network can increase processing effort without producing a defensible reference frame. The design balances coverage, geometry, uncertainty, field access and processing resources against the specific acceptance criteria.

Combining TLS with UAV photogrammetry, wearable LiDAR or conventional surveying can improve access to complementary surfaces. The integration is justified when each component supplies information needed by the final product and is validated at the relevant scale. It should not rely on the assumption that combining several dense clouds necessarily improves accuracy. Datum inconsistencies, correlated control errors and incompatible spatial resolution can persist in the merged dataset.

The examples demonstrate separate consequences of the measurement chain. Oblique incidence doubles the simplified spacing at 60° in the stated scenario. A 10 mm vertical bias over 1,000 m^2 produces a 10 m^3 volume difference. A 12.6 mm illustrative detection threshold prevents an 8 mm normal distance from being treated as significant under the assumed model. These are mathematical consequences of the selected inputs, not field evidence that a particular scanner meets those values.

The scope has deliberate limits. No scanner is ranked, no project-specific tolerance is prescribed and no experimental accuracy claim is made. The workflow still requires calibration information, actual control observations, independent tests and site-specific interpretation before operational use. Its practical value is to state what must be measured and checked so that the final model supports an engineering decision.

5. CONCLUSION

TLS provides three-dimensional observations of visible surfaces by combining range and angular measurements. Producing a reliable engineering model requires a defined measurand, a stable reference system, suitable scan geometry, controlled registration, task-specific surface reconstruction and independent validation. Point density,

internal registration residual and coordinate display precision cannot independently demonstrate the accuracy of the final product.

Terrain products require defensible ground classification, breaklines and a common domain for volume analysis. Slope products require full three-dimensional representation where necessary, stable multi-epoch control and uncertainty-aware change measurement. Complex geometries require multiple viewpoints, explicit handling of hidden surfaces and verification of mesh or parametric-model fidelity. Complementary sensors can extend coverage when their observations are tied to the same reference system and independently checked.

The technical workflow developed here connects these requirements to practical acceptance gates. Its analytical examples show how sampling geometry, datum bias and uncertainty affect deliverables without substituting calculated scenarios for experimental observations. Future site applications can implement this framework with recorded field settings, independent checkpoints and documented processing choices to obtain reproducible terrain, slope and object models.

Acknowledgements

No non-authorial contributions have been specified for this manuscript.

Funding

Funding information has not been supplied. The author should complete this declaration before submission.

Conflicts of interest

The author should confirm the conflict-of-interest declaration before submission.

Data availability statement

No new field dataset is reported. The numerical examples are reproducible from the assumed inputs and equations stated in the article. Published application contexts are identified in the references.

Institutional review board statement

Not applicable. The technical exposition does not involve human participants or animals.

CRediT author statement

Hacı Murat Yılmaz is the sole named author. The allocation of CRediT roles and approval of the final manuscript should be confirmed by the author before submission.

REFERENCES

[1] Alptekin, A., Çelik, M. Ö., & Yakar, M. (2019). Modelling of a sea cliff with terrestrial laser scanning. In *International Symposium on Applied Geoinformatics (ISAG-2019)* (pp. 199–202).

[2] Yakar, M., & Karabacak, A. (2023). *Giyilebilir mobil LiDAR ve uygulamaları*. Atlas Akademi. ISBN 978-625-8101-40-9.

[3] Karabacak, A., & Yakar, M. (2023). Incorrect use of wearable mobile LiDAR: Example of Mersin Soli Beach and Ankara National Library underpass. *Intercontinental Geoinformation Days, 7*, 234–237.

[4] Dörtbudak, E. B., & Akça, Ş. (2024). Comparing photogrammetry and smartphone LIDAR for 3D documentation: Kızılkoyun Necropolis case study. *Advanced LiDAR, 4*(1), 19–27.

[5] Yildiz, F., Karabork, H., Yakar, M., Altuntas, C., Karasaka, L., & Goktepe, A. (2007). 3D modelling by advanced total station. In *XXI International CIPA Symposium*, Athens, Greece.

[6] Koca, M., & Kozlu, H. H. (2021). Advantages and disadvantages of using TLS techniques in monumental buildings; Darsiyak Yanartaş Monastery Archangel Michael and Gabriel Church example. *Advanced LiDAR, 1*(1), 1–5.

[7] Albayrak, M., & Büyükmıhcı, G. (2021). Survey process of Gesi pigeonry with ground laser by (point cloud) scanning method. *Advanced LiDAR, 1*(1), 6–17.

[8] Güleç Korumaz, S. A. (2021). Terrestrial laser scanning with potentials and limitations for archaeological documentation: A case study of the Çatalhöyük. *Advanced LiDAR, 1*(1), 32–38.

[9] Besl, P. J., & McKay, N. D. (1992). A method for registration of 3-D shapes. *IEEE Transactions on Pattern Analysis and Machine Intelligence, 14*(2), 239–256. https://doi.org/10.1109/34.121791

[10] Zhang, W., Qi, J., Wan, P., Wang, H., Xie, D., Wang, X., & Yan, G. (2016). An easy-to-use airborne LiDAR data filtering method based on cloth simulation. *Remote Sensing, 8*(6), 501. https://doi.org/10.3390/rs8060501

[11] Kuçak, R. A., & Büyüksalih, İ. (2023). Comparison of CSF ground filtering method by using airborne LiDAR data. *Advanced LiDAR, 3*(2), 47–52.

[12] Sarıtaş, B., & Kaplan, G. (2023). Enhancing ground point extraction in airborne LiDAR point cloud data using the CSF filter algorithm. *Advanced LiDAR, 3*(2), 53–61.
[13] Sarıtaş, B., & Kaplan, G. (2024). Comprehensive study on enhanced accuracy analysis of LIDAR data: The example of Skopje. *Advanced LiDAR, 4*(1), 9–18.
[14] Fischler, M. A., & Bolles, R. C. (1981). Random sample consensus: A paradigm for model fitting with applications to image analysis and automated cartography. *Communications of the ACM, 24*(6), 381–395. https://doi.org/10.1145/358669.358692
[15] Kuçak, R. A. (2022). The feature extraction from point clouds using geometric features and RANSAC algorithm. *Advanced LiDAR, 2*(1), 15–20.
[16] Yakar, M., Yılmaz, H. M., & Mutluoğlu, Ö. (2008). *Lazer tarama teknolojisi ve fotogrametrik yöntem ile hacim hesabı* (Proje No. 105M179). TÜBİTAK.
[17] Abellán, A., Vilaplana, J. M., & Martínez, J. (2006). Application of a long-range terrestrial laser scanner to a detailed rockfall study at Vall de Núria (Eastern Pyrenees, Spain). *Engineering Geology, 88*(3–4), 136–148. https://doi.org/10.1016/j.enggeo.2006.09.012
[18] Yilmaz, H. M., Yakar, M., Yildiz, F., Karabork, H., Kavurmaci, M. M., Mutluoglu, O., & Goktepe, A. (2010). Determining rates of erosion of an earth pillar by terrestrial laser scanning. *Arabian Journal for Science and Engineering, 35*(2A), 163–172.
[19] Lague, D., Brodu, N., & Leroux, J. (2013). Accurate 3D comparison of complex topography with terrestrial laser scanner: Application to the Rangitikei canyon (N-Z). *ISPRS Journal of Photogrammetry and Remote Sensing, 82*, 10–26. https://doi.org/10.1016/j.isprsjprs.2013.04.009
[20] Promneewat, K., & Taksavasu, T. (2024). Performance of affordable 2D cave scanning technique from LiDAR for constructing 3D cave models. *Advanced LiDAR, 4*(1), 1–8.
[21] Kanun, E., Alptekin, A., & Yakar, M. (2021). 3D ship modeling with laser scanning method. In *Proceedings of the International Symposium on Applied Geoinformatics (ISAG2021)*, Riga, Latvia, 2–3 December. https://doi.org/10.15659/isag2021.12314
[22] Özeren, Ö., & Korumaz, M. (2021). Lidar to HBIM for analysis of historical buildings. *Advanced LiDAR, 1*(1), 27–31.
[23] Karabork, H., Yildiz, F., Yakar, M., Altuntas, C., & Karasaka, L. (2007). Modeling and visualization using laser scanner in documentation of cultural heritage. In *XXI International CIPA Symposium*, Athens, Greece.
[24] Goktepe, A., Karabork, H., Yakar, M., Yildiz, F., & Baygul, E. (2009). 3D modeling of Sille Aya-i Eleni Church with laser technology. In *22nd CIPA Symposium—Digital Documentation, Interpretation & Presentation of Cultural Heritage*, Kyoto, Japan.
[25] Güleç Korumaz, A., Korumaz, M., Dülgerler, O. N., Karasaka, L., Yildiz, F., & Yakar, M. (2010). Evaluation of laser scanner performance in documentation of historical and architectural ruins, a case study in Konya. *International Archives of Photogrammetry, Remote Sensing and Spatial Information Sciences, 38*(Part 5), 361–366.
[26] Çelik, M. Ö., Alptekin, A., & Yakar, M. (2019). Modelling of the mausoleum in Kanlidivane ruins with terrestrial laser scanner. In *2nd International Mersin Symposium*, Mersin, Türkiye, 23–25 May.
[27] Köse, S., & Us, H. (2023). Application of terrestrial laser scanning (TLS) technology for documentation of cultural heritage buildings and structures: A case study Sarı İsmail Sultan Tomb. *Advanced LiDAR, 3*(1), 35–40.
[28] Kanun, E., Metin, A., & Yakar, M. (2021). Yersel lazer tarama tekniği kullanarak Ağzıkara Han'ın 3 boyutlu nokta bulutunun elde edilmesi. *Türkiye Lidar Dergisi, 3*(2), 58–64. https://doi.org/10.51946/melid.1025856
[29] Karataş, L., Alptekin, A., & Yakar, M. (2023). Investigating the material deteriorations on the facades of stone structures by terrestrial laser scanning method: Case study of Mardin mansion. *Afyon Kocatepe Üniversitesi Fen ve Mühendislik Bilimleri Dergisi, 23*(3), 700–711. https://doi.org/10.35414/akufemubid.1197891
[30] Alyilmaz, C., Alyilmaz, S., & Yakar, M. (2010). Measurement of petroglyhps (rock of arts) of Qobustan with close range photogrammetry. *International Archives of Photogrammetry, Remote Sensing and Spatial Information Sciences, 38*(Part 5), 29–32.
[31] Kaderli, L. (2021). Documentation methods from tradition to the present: Case study Cappadocia. *Advanced LiDAR, 1*(1), 18–26.
[32] Özdemir, İ., & Güngör, A. (2024). Documentation of archaeological excavation sites with terrestrial laser scanning and UAV photogrammetry methods. *Advanced LiDAR, 4*(1), 28–32.